RJ 10167 (95042) November 18, 1999
Magnetic Recording

00A000024

# Research Report

## AN ANALYTIC MODEL OF MR/GMR HEAD SENSITIVITY FUNCTION

Martin Hassner

IBM Research Division
Almaden Research Center
650 Harry Road
San Jose, CA 95120-6099

Dr. D. V. Leykin

Theoretical Physics Division
NASU Institute of Magnetism
36-B Vernadsky Street
Kiev-680, 252142
Ukraine

Tobin A Driscoll

Dept. of Applied Mathematics, CB 526
University of Colorado
Boulder, CO 80309-0526

RJ 10167 (95042) November 18, 1999
Magnetic Recording



## 1. Abstract

We describe the calculation of an analytic model of the MR/GMR head sensitivity function for variable flying heights. This model makes use of the analytic inversion of the Schwarz-Christoffel integral for the MR/GMR head geometry conformal map. The analytic inversion makes use of elliptic functions which uniformize the conformal map.

CONTENTS

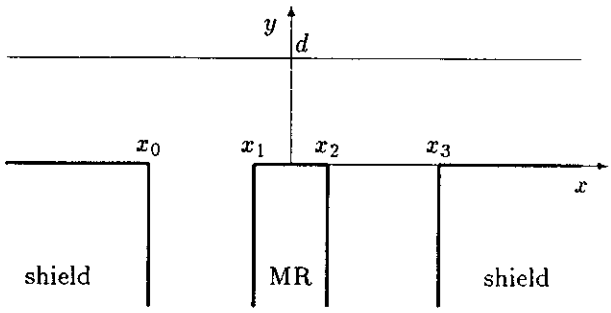


FIGURE 1. Model geometry.

## 1. MATHEMATICAL MODEL OF READ-BACK PROCESS

For head geometry we assume the setup shown on Figure 1. Origin of coordinate system is centered on MR element. Dimensions $x_1 - x_0 = G_1$, $x_2 - x_1 = 2\ell$ and $x_3 - x_2 = G_2$ form the essential set of parameters.

Permeability of MR element and shields is assumed to be $\infty$, permeability is set 1, medium is assumed infinitely thin, width of track and head is assumed to be $\infty$.

We assume the following model of read-back process of magnetic signals. Normalized output voltage $V(vt)$, where $t$ is time and $v$ is linear velocity, of a MR head on fly height $d$ is given by [1, 2, 3]:

$$V(vt) = \Phi\left(\int_{-\infty}^{+\infty} \mathrm{d}z H(z) \frac{\partial m(z - (vt + \imath d))}{\partial z}\right), \tag{1}$$

where $m(z)$ is the *magnetization distribution* in recording medium; $H(z)$ is the *sensitivity function* of the head, which is magnetostatic potential defined by boundary conditions $\Re H(z) = 1$ on MR and $\Re H(z) = 0$ on shields (see Figure 1); $\Phi$ is so-called *transfer function* of the MR element. Functions $m$ and $H$ here are complex-analytic functions of variable $z = x + \imath y$. Integration is carried out along the real line $y = 0$.

The equation (1) describes major counterparts of read-back process. Function $\Phi$ models the nonlinearity of magneto-resistive effect. Function $H(z)$ is completely defined by parameters $G_1, G_2, \ell$ and accounts for influence of head geometry on read-back shape and spectral properties.

It is the sensitivity function of head $H(z)$ which is the subject of our interest here. Importance of this object follows from the fact, that response to a single transition of shape $m(z) = \frac{1}{\pi} tan^{-1}(x/a)$ in medium with purely horizontal magnetization is equal to $S(z + \imath a)$ (see, e.g., [3]).

Note, that as $H(x+\imath d)$ is related to $H(x)$, the magnetostatic potential on contact line of the head, by

$$H(x + \imath d) = \frac{1}{2\pi\imath} \int_{-\infty}^{+\infty} \mathrm{d}x' \frac{H(x')}{x' - (x + \imath d)},$$

we may rewrite the equation (1) in terms of Fourier transform $\mathcal{F}$ and Hilbert transform $\mathcal{H}$ (transform $\mathcal{H}$ acts on Fourier image $\widetilde{f}(\omega)$ of a real-valued function $f(x)$ by $\mathcal{H} : \widetilde{f}(\omega) \mapsto 2U(\omega)\widetilde{f}(\omega)$, where $U$ is unit step function, so that $\mathcal{F}^{-1}(\mathcal{H}(\widetilde{f}))$ is a

complex-analytic function whose real part is $f(x)$) as follows:

$$V(vt) = \Phi\Big(\mathcal{F}^{-1}\big(\mathcal{H}\big(e^{-d|\omega|}h(\omega)\big)\widetilde{m}(\omega)\big)\Big), \tag{2}$$

where $\widetilde{m} = \mathcal{F}(m)$ and $\widetilde{h}$ is Fourier transform of $h(x) = \Re H(x)$. So, construction of the sensitivity function of a head reduces to building the corresponding function $\widetilde{h}$.

The function $h(x)$ is a piece-wise function

$$h(x) = \begin{cases} 0, & x \le x_0 \\ f_1\left(\frac{x-x_0}{x_1-x_0}\right), & x_0 < x \le x_1 \\ 1, & x_1 < x \le x_2 \\ f_2\left(\frac{x-x_3}{x_2-x_3}\right), & x_2 < x \le x_3 \\ 0, & x_3 < x \end{cases}; \tag{3}$$

note, that functions $f_1$ and $f_2$ take their arguments and values in $[0, 1]$, and are monotonously increasing functions. We will call these functions *normalized potentials*.

In the following sections we derive approximation of $f_i(x)$ based on implicit solution of boundary value problem defining $H(x+\imath y)$ in terms of elliptic functions (parametrisation of Schwarz-Christoffel map). The approximation is an analogue of two-point Pade approximation and its accuracy may be improved to arbitrary prescribed level. Along with exposition, we apply the technique developed to the running example of the case of geometry defined by $G_1 = 777\text{Å}$, $G_2 = 559\text{Å}$ and $\ell = 36\text{Å}$. Finally, we single out primitive building blocks of $\widetilde{h}$, and give an approximation of it based on Pade-type approximation of $h(x)$.

## 2. Elliptic model

Magnetostatic potential $H(z)$ defined by boundary conditions $\Re H(z) = 1$ on MR and $\Re H(z) = 0$ on shields is found with the help of standard conformal Schwarz-Christoffel map

$$z(w) = C_0 + C_1 \int_w^\infty \mathrm{d}t \frac{\sqrt{4t^3 - g_2 - g_3}}{(t-\beta)^2(t-\chi_1)(t-\chi_2)}, \tag{4}$$

as follows:

$$H(z) = \frac{1}{\imath\pi} \log\Big(\frac{w(z)-\chi_1}{w(z)-\chi_2} \cdot \frac{\beta-\chi_2}{\beta-\chi_1}\Big). \tag{5}$$

Formulation of the boundary value problem follows [4, 3].

Real parameters $C_0, C_1, g_2, g_3, \beta, \chi_1$ and $\chi_2$ in (4) are derived from correspondence of boundaries

$$\begin{array}{llll} z(\beta) = \infty, & z(\chi_1) = -\imath\infty, & z(\chi_2) = -\imath\infty, & \\ z(\infty) = x_0, & z(e_1) = x_1, & z(e_3) = x_2, & z(e_2) = x_3, \end{array}$$

where $e_1 > e_2 > e_3$ are roots of $4t^3 - g_2 - g_3$. This is done numerically once for each geometry. Dr. T. Driscoll created a *Mathlab* toolbox which calculates the required set of parameters of the Schwarz-Christoffel map given head dimensions.

Formula (5) implies *inversion* of the map (4), which is currently not known explicitly in closed form. However, using elliptic functions [5, 6], we can achieve

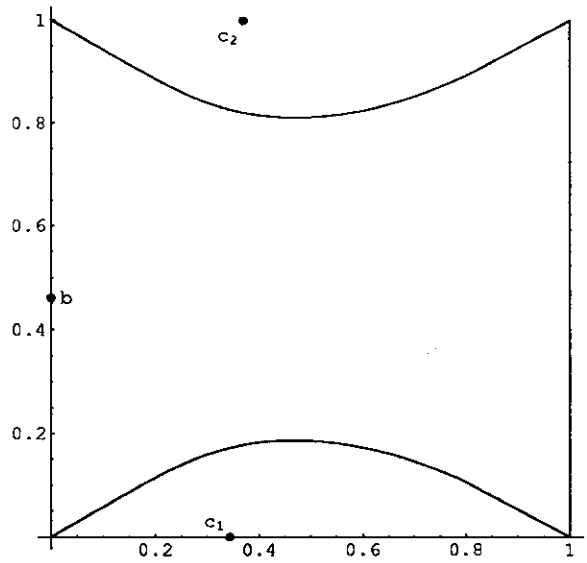


FIGURE 2. Preimage of contact line of the head in the plane of variable $u = x\omega_1 + y\omega_2$; with $\{\omega_1, \omega_2\}$ being half-periods of elliptic function $\wp$.

*explicit uniformization* of both (5) and (4) by complex parameter $u$ residing in a rectangle in complex plane. Put $w = \wp(u)$, we obtain

$$
\begin{aligned}
z(u) &= Q_1\left(\log\frac{\sigma(c_1+u)}{\sigma(c_1-u)} - 2u\zeta(c_1)\right) + Q_2\left(\log\frac{\sigma(c_2+u)}{\sigma(c_2-u)} - 2u\zeta(c_2)\right) \\
&\quad + Q_3\big(\zeta(b+u) - \zeta(b-u) + 2u\wp(b)\big), \qquad (6) \\
H(u) &= \frac{1}{\imath\pi}\log\Big(\frac{\wp(u)-\chi_1}{\wp(u)-\chi_2}\cdot\frac{\beta-\chi_2}{\beta-\chi_1}\Big),
\end{aligned}
$$

where $\sigma$, $\zeta$ and $\wp$ are Weierstrass elliptic functions of invariants $g_2$ and $g_3$; and also $c_1 = \wp^{-1}(\chi_1)$, $c_2 = \wp^{-1}(\chi_2)$ and $b = \wp^{-1}(\beta)$; constants $Q_1 = \frac{G_1}{\imath\pi}$ $Q_2 = \frac{G_2}{\imath\pi}$ and $Q_3 = \frac{1}{\imath\pi}(2\ell\omega_1 - G_1c_1 - G_2\Re c_2)$, where $\omega_1$ is real half-period of $\wp$.

The elliptic parametrisation (6) may serve as a source of various kinds of approximations for the dependence $H = H(z)$. In the present work we also use it to obtain numerical data to anchor analytical results.

For our example we have:

$$
\begin{aligned}
&g_2 = 1.00001, && g_3 = 0.00145192 \\
&c_1 = 0.63524, && c_2 = 0.68469 + 1.85592\imath, \qquad b = 0.85598\imath.
\end{aligned}
$$

Figure 2 shows the path in plane of uniformizing parameter $u$ of elliptic model (6) which corresponds to contact line $y = 0$ for the geometry considered.

Figure 3 shows profile of $h(x)$ on the contact line of the head.

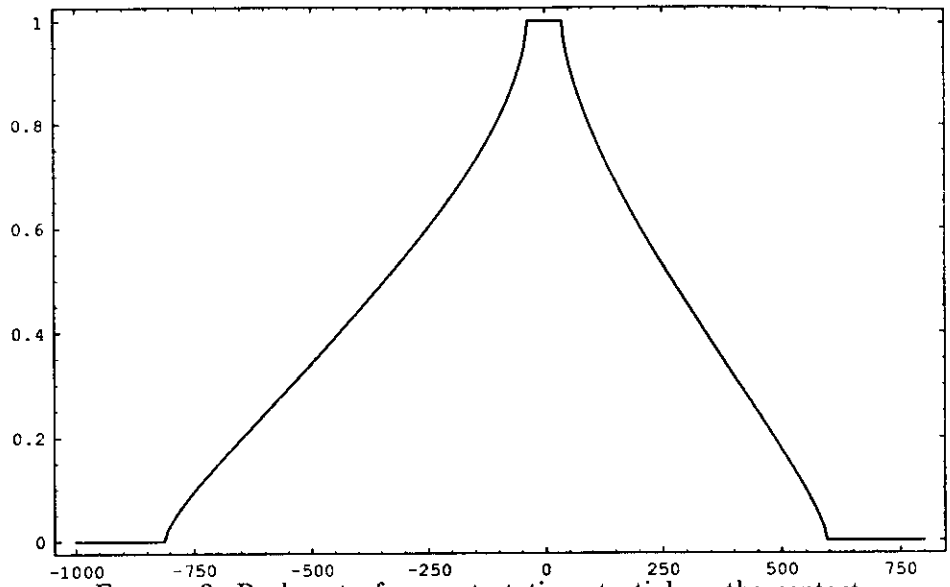


FIGURE 3. Real part of magnetostatic potential on the contact line of the head.

## 3. POWER SERIES REPRESENTING NORMALIZED POTENTIALS NEAR $t = 0$ AND $t = 1$

Our subject here is derivation of series representing $f_1(t)$ and $f_2(t)$ near the corners of the head.

Using equations (4) and (5), or, equivalently, from (6), we derive power series expansions of the function $H(z)$ near points $x_i$ for $i = 0, 1, 2, 3$ in the form:

$$H(z) \cong \mathfrak{P}_i(z - x_i) = \sum_{k=0}^{\infty} A_k^{(i)} (z - x_i)^{k/3}.$$

This kind series is a result of formal series inversion of, say, (4), and composition with formal series of (5). Relevance of such series is limited to immediate vicinity of points $x_i$. Important advantage of series $\mathfrak{P}_i$ is that coefficients $A_k^{(i)}$ are, in principle, known to be explicit functions of parameters $G_1, G_2, \beta, \chi_1, \chi_2, g_2$ and $g_3$ for all $k = 0, 1, 2, \ldots$.

By taking real part of series $\mathfrak{P}_0(\frac{z-x_0}{x_1-x_0})$ and $\mathfrak{P}_1(\frac{z-x_1}{x_0-x_1})$, after the change of variable by $t = \frac{z-x_0}{x_1-x_0}$, we obtain a pair of series for $f_1(t)$ near $t = 0$ and $t = 1$:

$$f_1(t) \cong \mathfrak{p}_0^{(1)}(t) = \sum_{i=0}^{\infty} a_{6i+2}^{(1)} t^{(6i+2)/3} + a_{6i+4}^{(1)} t^{(6i+4)/3} =$$

$$(7) \qquad a_2^{(1)} t^{2/3} + a_4^{(1)} t^{4/3} + a_8^{(1)} t^{8/3} + a_{10}^{(1)} t^{10/3} + a_{14}^{(1)} t^{14/3} + \ldots;$$

$$f_1(t) \cong \mathfrak{p}_1^{(1)}(1-t) = 1 + \sum_{i=0}^{\infty} b_{6i+2}^{(1)} (1-t)^{(6i+2)/3} + b_{6i+4}^{(1)} (1-t)^{(6i+4)/3} =$$

$$1 + b_2^{(1)} (1-t)^{2/3} + b_4^{(1)} (1-t)^{4/3} + b_8^{(1)} (1-t)^{8/3} + b_{10}^{(1)} (1-t)^{10/3} + \ldots;$$

Clearly, for the function $f_2$ we have a similar pair of expansions $\{\mathfrak{p}_0^{(2)}(t), \mathfrak{p}_1^{(2)}(1-t)\}$.

Let us give explicit expressions for first few of the coefficients $a_i^{(1)}$ and $b_i^{(1)}$.

$$a_2^{(1)} = \frac{\sqrt{3}}{4}\left[\frac{9(4\chi_1^3 - g_2\chi_1 - g_3)(\chi_1 - \chi_2)}{2\pi(\chi_1 - \beta)^4}\right]^{1/3};$$

$$a_4^{(1)} = -\frac{3\sqrt{3}}{2^5 5}\left[\frac{6\pi(4\chi_1^3 - g_2\chi_1 - g_3)^2}{(\chi_1 - \chi_2)(\chi_1 - \beta)^8}\right]^{1/3} \times (8\beta - \chi_1 - \chi_2);$$

$$a_8^{(1)} = \frac{\sqrt{3}}{2^8 5^3 7}\left[\frac{9\pi^5(4\chi_1^3 - g_2\chi_1 - g_3)^4}{2(\chi_1 - \chi_2)^5(\chi_1 - \beta)^{16}}\right]^{1/3} \times$$
$$\left[4\beta\{3127\beta^2 + 2298\beta(\chi_1 + \chi_2) + 69(\chi_1 + \chi_2)^2 - 25(\chi_1 - \chi_2)^2\} + \right.$$
$$\left. 25g_2\{128\beta + 19(\chi_1 + \chi_2)\} + \frac{1}{2}\{25(\chi_1 + \chi_2)(\chi_1 - \chi_2)^2 - 23(\chi_1 + \chi_2)^3\} - 875g_3\right];$$

$$b_2^{(1)} = \frac{3^{7/6}}{2^{5/3}\pi}\xi_1 q^{1/3};$$

$$b_4^{(1)} = -\frac{3^{4/3}}{2^{1/3}20\pi}(2\kappa\xi_1 - 5\xi_2)q^{2/3}; \tag{8}$$

$$b_8^{(1)} = \frac{3^{5/3}}{2^{2/3}700\pi}\big((1078\kappa^3 - 1650\kappa\lambda)\xi_1 +$$
$$(1500\lambda - 2310\kappa^2)\xi_2 + 3150\kappa\xi_3 - 2625\xi_4\big)q^{4/3};$$

where

$$\xi_n = \frac{1}{n}\left(\frac{1}{(e_1 - \chi_2)^n} - \frac{1}{(e_1 - \chi_1)^n}\right);$$

$$\kappa = \frac{6e_1}{12e_1^2 - g_2} - \frac{2}{e_1 - \beta} - \frac{1}{e_1 - \chi_1} - \frac{1}{e_1 - \chi_2};$$

$$\lambda = -\frac{3g_2}{2(12e_1^2 - g_2)^2} + \frac{3}{(e_1 - \beta)^2} + \frac{1}{(e_1 - \chi_1)^2} + \frac{1}{(e_1 - \chi_2)^2} - \tag{9}$$
$$\frac{\beta + 23e_1}{2(12e_1^2 - g_2)(e_1 - \beta)} - \frac{6e_1}{(12e_1^2 - g_2)(e_1 - \chi_1)} - \frac{6e_1}{(12e_1^2 - g_2)(e_1 - \chi_2)} +$$
$$\frac{5e_1 - \beta - 2\chi_1 - \chi_2}{(e_1 - \beta)(e_1 - \chi_1)(e_1 - \chi_2)};$$

$$q = \pi^2\frac{(4\chi_1^3 - g_2\chi_1 - g_3)(e_1 - \beta)^4(e_1 - \chi_1)^2(e_1 - \chi_2)^2}{(12e_1^2 - g_2)(\chi_1 - \beta)^4(\chi_1 - \chi_2)^2}.$$

Formulas for $a_i^{(2)}$ and $b_i^{(2)}$ are similar to (8). Namely, first change places of $\chi_1$ and $\chi_2$ in the expression for $q$, then formulas for $a_i^{(2)}$ are obtained from (8) by substituting $e_3$ in place of $e_1$ in (9), and for $b_i^{(2)}$ using $e_2$ instead of $e_1$.

Further coefficients become very cumbersome. Nevertheless, we believe, that for practical purposes the set of formulas given here is sufficient.

In the sample case we have:

$$\mathfrak{p}_0^{(1)}(t) = 0.4389795t^{2/3} + 0.3333486t^{4/3} + 0.00113887t^{8/3} + 0.05551831t^{10/3} + O(t^{14/3});$$
$$\mathfrak{p}_1^{(1)}(t) = 1 - 1.1078091t^{2/3} + 0.6448524t^{4/3} - 5.4354796t^{8/3} - 17.4507645t^{10/3} + O(t^{14/3}).$$

Though convergence of this series is not a question of our primary interest here, let us indicate how to determine convergence radius $\rho$ is determined for example for the series $\mathfrak{p}_0^{(1)}(t)$. To do this we have to find a point on the path shown on Figure 2 such that $|u_c| = \sqrt{x_c^2\omega_1^2 - y_c^2\omega_2^2} = \min(|c_1|, |b|)$, then $\rho = \frac{z(u_c)-x_0}{G_1} < 1$, where $z(u)$ is as in (6).

## 4. Pade-type approximations of normalized potentials

Similarly to standard approach of the theory of Pade approximations we introduce an object $P(\mathfrak{p}_0^{(1)}(t), \mathfrak{p}_1^{(1)}(1-t); n)$ which combines analytical information contained in both series $\mathfrak{p}_0^{(1)}(t)$ and $\mathfrak{p}_1^{(1)}(1-t)$ in such a way, that expansions of $P(\mathfrak{p}_0^{(1)}(t), \mathfrak{p}_1^{(1)}(1-t); n)$ near $t = 0$ and $t = 1$ coincide with each of the corresponding series up to order $(n+1)/3$. Such an object is realized by formula:

$$P(\mathfrak{p}_0^{(1)}(t), \mathfrak{p}_1^{(1)}(1-t); n) = \frac{\sum_{i=0}^{n} \alpha_i t^{i/3}(1-t)^{(n-i)/3}}{\sum_{i=0}^{n} \beta_i t^{i/3}(1-t)^{(n-i)/3}}; \tag{10}$$

One repeats without any substantial change standard argument to determine coefficients $\alpha_i$ and $\beta_i$: truncating expansions

$$\sum_{i=0}^{n} \alpha_i t^{i/3}(1-t)^{(n-i)/3} - \mathfrak{p}_0^{(1)}(t) \sum_{i=0}^{n} \beta_i t^{i/3}(1-t)^{(n-i)/3}$$

near point $t = 0$ at $O(t^{(n+1)/3})$ and

$$\sum_{i=0}^{n} \alpha_i t^{i/3}(1-t)^{(n-i)/3} - \mathfrak{p}_1^{(1)}(1-t) \sum_{i=0}^{n} \beta_i t^{i/3}(1-t)^{(n-i)/3}$$

near $t = 1$ at $O((1-t)^{(n+1)/3})$ and equating coefficients at fractional powers of $t$ and $1-t$ one obtains a system of homogeneous linear equations whence coefficients $\alpha_i$ and $\beta_i$ are determined up to common constant factor.

For our running example we have:

$$P(\mathfrak{p}_0^{(1)}(t), \mathfrak{p}_1^{(1)}(1-t); 7) = [0.470097(1-t)^{5/3}t^{2/3} + 0.420875(1-t)^{4/3}t + 0.428214(1-t)t^{4/3} + 0.869416(1-t)^{2/3}t^{5/3} - 0.074970(1-t)^{1/3}t^2 + t^{7/3}]/[1.07089(1-t)^{7/3} + 0.95875(1-t)^2t^{1/3} + 0.16227(1-t)^{5/3}t^{2/3} + 1.96641(1-t)^{4/3}t + 0.34516(1-t)t^{4/3} + 1.97723(1-t)^{2/3}t^{5/3} - 0.07497(1-t)^{1/3}t^2 + t^{7/3}]$$

Figure 4 shows plot of this function together with numerical data for the function $f_1$. There are 101 distinct equally spaced dots over unit interval, representing the numerical data, and these dots cover the curve; so it is visible that absolute accuracy

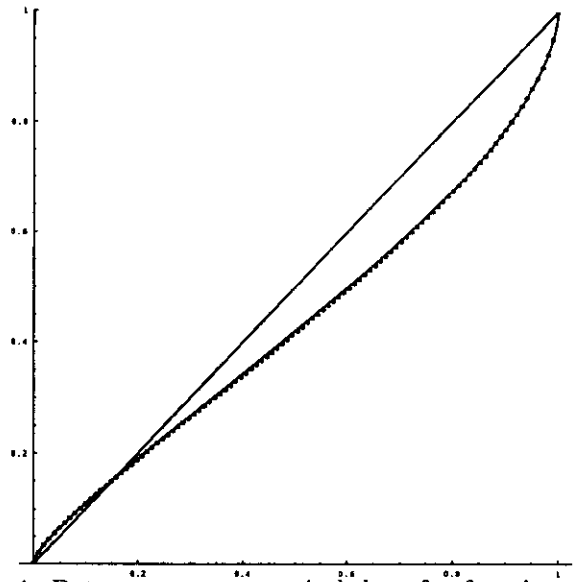

FIGURE 4. Dots represent numerical data for function $f_1$; solid curve is the plot of $P(\mathfrak{p}_0^{(1)}(t), \mathfrak{p}_1^{(1)}(1-t); 7)$; straight line shows Karlquist-Potter approximation.

of this approximation is at least within 1%. Note, that we actually used only two nontrivial terms in each of the expansions to derive this approximation.

It remains to say here that uniqueness of representation (10) and the fact that $f_1(t) = \lim_{n\to\infty} P(\mathfrak{p}_0^{(1)}(t), \mathfrak{p}_1^{(1)}(1-t); n)$ follows by standard argument from existence of global elliptic uniformization (6), uniqueness of Taylor series and possibility of analytic extension along the path shown on Figure 2.

## 5. FOURIER TRANSFORM OF $h(x)$

From decomposition (3) we have:

$$\widetilde{h}(\omega) = \int_{x_0}^{x_1} \mathrm{d}x \exp\{\omega x\} f_1\left(\frac{x-x_1}{x_1-x_0}\right) + \int_{x_1}^{x_2} \mathrm{d}x \exp\{\omega x\} + \int_{x_2}^{x_3} \mathrm{d}x \exp\{\omega x\} f_2\left(\frac{x-x_3}{x_2-x_3}\right).$$

So, as $x_0 = -\ell - G_1$, $x_1 = -\ell$, $x_2 = \ell$ and $x_3 = G_2 + \ell$, we have

$$\widetilde{h}(\omega) = \frac{2\sin(\ell\omega)}{\omega} + G_1 \exp\{-\omega(G_1+\ell)\} \int_0^1 \mathrm{d}t \exp\{\omega G_1 t\} f_1(t) - G_2 \exp\{\omega(G_2+\ell)\} \int_0^1 \mathrm{d}t \exp\{-\omega G_2 t\} f_2(t);$$

we are going to replace in this formula normalized potentials $f_1$ and $f_2$ by their approximations (10).

Let $F_1(t) = P(\mathfrak{p}_0^{(1)}(t), \mathfrak{p}_1^{(1)}(1-t); n)$ be the approximation of $f_1(t)$, substituting $t = \frac{s^3}{1+s^3}$ we obtain $F_1(\frac{s^3}{1+s^3}) = \frac{P_1(s)}{Q_1(s)}$ where $P_1$ and $Q_1$ are polynomials of degree

$n$ with real coefficients. Let $\{r_1^{(1)}, \ldots, r_n^{(1)}\}$ be roots of $Q_1$, then we have primitive fraction decomposition:

$$F_1\Big(\frac{s^3}{1+s^3}\Big) = \frac{P_1(s)}{Q_1(s)} = R_0^{(1)} + \sum_{i=1}^{n} \frac{R_i^{(1)}}{s - r_i^{(1)}},$$

where $R_0^{(1)} = \lim_{s\to\infty} \frac{P_1(s)}{Q_1(s)} = f_1(1) = 1$ and $R_i^{(1)} = \frac{P_1(r_i^{(1)})}{Q_1'(r_i^{(1)})}$ for $i = 1, \ldots, n$. Therefore:

$$\int_0^1 \mathrm{d}t \exp \imath\omega t f_1(t) \sim \imath\frac{1 - e^{\imath\omega}}{\omega} + \sum_{i=1}^{n} R_i^{(1)} K(\omega, r_i^{(1)}),$$

where

$$K(\omega, \alpha) = \int_0^1 \mathrm{d}t \exp \imath\omega t \frac{(1-t)^{1/3}}{t^{1/3} - \alpha(1-t)^{1/3}} = \sum_{m=0}^{\infty} k_m(\alpha) \frac{(\imath\omega)^m}{m!} \tag{11}$$

with coefficients $k_j(\alpha)$ defined by recursion

$$k_{j+1}(\alpha) = -\tfrac{\alpha^3}{1-\alpha^3} k_j(\alpha) - \tfrac{1}{1-\alpha^3}\Big(\tfrac{\alpha^2}{(n+1)(n+2)} + \tfrac{\Gamma(\frac{4}{3})\Gamma(j+\frac{5}{3}) - \alpha\Gamma(j+\frac{4}{3})\Gamma(\frac{5}{3})}{(n+2)!}\Big)$$

for $j > 0$ and $k_0(\alpha) = \frac{2\pi}{3\sqrt{3}} \frac{1-\alpha^2}{(1+\alpha+\alpha^2)^2} - \frac{\alpha^2}{(1-\alpha^3)}(1 + 3\frac{\log(\alpha)}{1-\alpha^3})$.

The function $K(\omega, \alpha)$ is defined by (11) for all $\omega \in \mathbb{C}$ and $\alpha \in \mathbb{C}\backslash\{0, 1, e^{\pm 2\imath\pi/3}\}$.

Finally, we have derived an approximation of $\widetilde{h}(\omega)$ in the form:

$$\widetilde{h}_{\mathrm{approx}}(\omega) = \frac{2\sin(\ell\omega)}{\omega} + \frac{2\sin(G_1\omega/2)}{\omega} e^{-\imath\omega(\ell + \frac{G_1}{2})} + \frac{2\sin(G_2\omega/2)}{\omega} e^{\imath\omega(\ell+\frac{G_2}{2})} + G_1 e^{-\imath\omega(G_1+\ell)} \left[\sum_{i=1}^{n} R_i^{(1)} K(G_1\omega, r_i^{(1)})\right] + G_2 e^{\imath\omega(G_2+\ell)} \left[\sum_{i=1}^{n} R_i^{(2)} K(-G_2\omega, r_i^{(2)})\right]. \tag{12}$$

Roots $r_i^{(2)}$ and residues $R_i^{(2)}$ of approximation $F_2(t) = P(\mathfrak{p}_0^{(2)}(t), \mathfrak{p}_1^{(2)}(1-t); n)$ are defined in the same way as $r_i^{(1)}$ and $R_i^{(1)}$ above.

For our toy model using (12) with series (11) truncated after linear in $\omega$ term, then for fly height $d = 200\text{Å}$ by inverse Fourier transform $H_{\mathrm{approx}}(x + \imath d) = \frac{1}{2\pi}\int_{-\infty}^{\infty} \mathrm{d}\omega e^{-\imath\omega x - d|\omega|} \widetilde{h}_{\mathrm{approx}}(\omega)$ we obtain an approximation of $H(x + \imath d)$ of the form

$$H_{\mathrm{approx}}(x + \imath d) = \sum_{i=0}^{3} A_i \log[x - x_i + \imath d] + \frac{B_i}{x - x_i + \imath d},$$

with some complex constants $A_i$ and $B_i$. The result is shown on Figures 5 and 6. One have to use more terms in (11) as the fly height decreases for such kind of approximation, provided choice of oder in (10) is optimal.

## 6. Aprroximation of $H(z)$

Above we proposed an approximation of the real part $h(x)$ of magnetostatic potential along the contact line of head, which by standard formula

$$H(z) = \frac{1}{\imath\pi} \int_{-\infty}^{\infty} \mathrm{d}x \frac{h(x)}{x - z}, \qquad \Im z \geq 0,$$

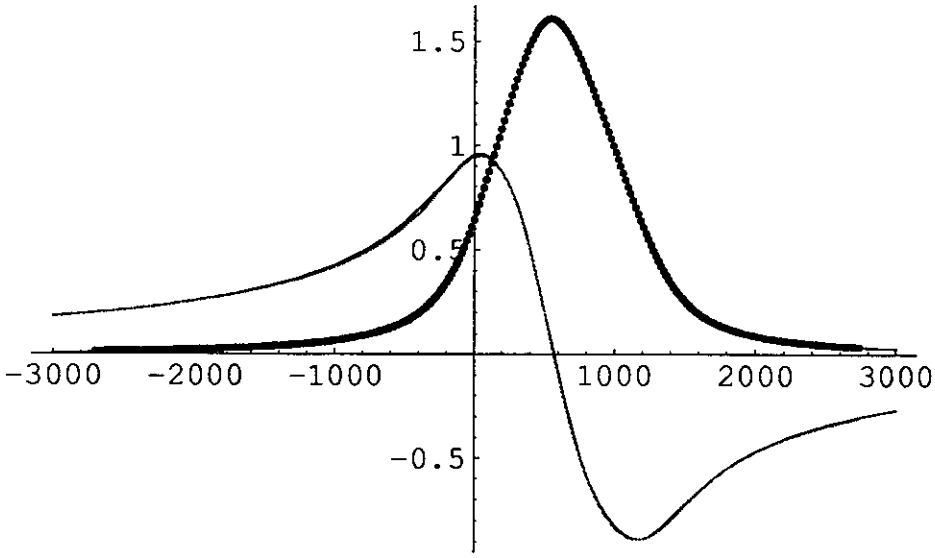


FIGURE 5. Real and imaginary parts of $H_{\text{approx}}(x + id)$, dots represent numerical data, red lines represent parametric plot of $\pi H(x + id)$ by (6).

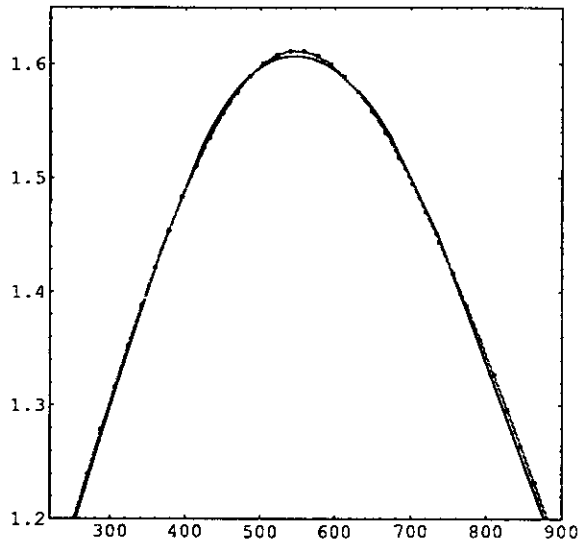


FIGURE 6. Zoom of Figure 5 near peak of the real part of $\pi H(x + id)$.

is globalized to upper half-plane. Using roots $r_i^{(1,2)}$ and residues $R_i^{(1,2)}$, associated with approximation as we did in the previous section, we obtain, for MR or GMR head with dimensions $G_1 : 2\ell : G_2$, the following expression for approximate

sensitivity function:

$$H_{\text{approx}}(z) = \frac{1}{\imath\pi}\log\frac{\ell+G_2-z}{\ell+G_1+z} + \left[\sum_{i=1}^{n}\imath R_i^{(1)}\varphi\left(\tfrac{G_1+\ell+z}{G_1}, r_i^{(1)}\right)\right] + \left[\sum_{i=1}^{n}\imath R_i^{(2)}\varphi\left(\tfrac{G_2+\ell-z}{G_2}, r_i^{(2)}\right)\right],$$

where

$$\varphi(\xi,\alpha) = \frac{1}{\pi}\int_0^1 \mathrm{d}t\frac{1}{\xi-t}\cdot\frac{(1-t)^{1/3}}{t^{1/3}-\alpha(1-t)^{1/3}} = \frac{1}{\sqrt{3}(1+\alpha+\alpha^2)} - \frac{\xi^{1/3}(\xi-1)^{1/3}(\xi^{1/3}-(1-\xi)^{1/3}\alpha)}{\sqrt{3}(\xi-\alpha^3(\xi-1))} + \frac{\alpha^2(\xi-1)}{\pi(\xi-\alpha^3(\xi-1))}\log(\xi(\xi-1)).$$

This approximation is valid in the whole upper half-plane of variable $z$ except for a finite set of points (which may appear to be empty).

## 7. On processing of test stand data

Test stand data are arrays $V$ of real numbers of length $N$, representing output voltage digitized at some linear velocity $v$ with some time resolution $T$. If the inverse transfer function $\Phi^{-1}$ is known, we may use equation (2) in order to recover distribution of magnetization $m(z)$. To do this we have to replace Fourier transform $\mathcal{F}$ be Discrete Fourier transform dft and continuous operation of convolution, which is just multiplication of Fourier images, by its discrete analog. Discrete operation convolution is formalized as multiplication of polynomials. Namely, dft converts set of samples $S = \{s_1, \ldots, s_N\}$ to a set of frequency samples $F = \{f_0, f_1, \ldots, f_N\}$; convolution $S$ of such sets $S$ and $S'$ is $\mathrm{dft}^{-1}$ of the set of frequency samples $F''$ which is equal to the set of coefficients of the polynomial $p(F'')(t) = p(F)(t)p(F')(t)$, in a formal parameter $t$, where $p(F)(t) = \sum_{i=0}^{N} f_i t^i$, etc. Inverse of convolution is division of corresponding polynomials. In this notation:

$$p(\mathrm{dft}\Phi^{-1}(V))(t) = p(\mathrm{dft}H)(t)p(\mathrm{dft}m)(t),$$

where $H$ and $m$ denote sets of samples of sensitivity function and magnetization, properly aligned with $V$. We can invert

$$p(\mathrm{dft}m)(t) = \frac{p(\mathrm{dft}\Phi^{-1}(V))(t)}{p(\mathrm{dft}H)(t)}, \tag{13}$$

and, if length of array $H$ is $M$, recover $N-M$ frequency samples of $m$. For this operation to make any sense, some restriction must be put on data. All three of the numbers $N$, $M$ and $N-M$ should be large enough in order that operation (13) would be meaningful; as $M$ is at our disposal it seems reasonable to chose $M \cong N/2$. The set of samples $V$ has to be spatially dense, that is, $\Delta = vT$ has to be at least of the same order of magnitude as width of MR element $2\ell$.

For the head which was our example above we know the inverse transfer function as empiric equation $\Phi^{-1}(A) = A + X_1A^2 + X_2A^3$, with constants $X_1 = 0.6544$ and $X_2 = 6.5493$. But, unfortunately, the sets of data available on this stage of project (see Figure 7) are not satisfactory. The samples were digitized with time resolution of $T = 1\text{ns}$. Linear velocity was 47.7 m/s. This makes $\Delta = 477\text{Å} \cong 13.25\ell$. Data were written at 20 Mflux/s with 20 spaces between patterns. Roughly, we have 50 samples for a pattern. As $N$ is equal to 50, we have to set $M = 25$. This means that

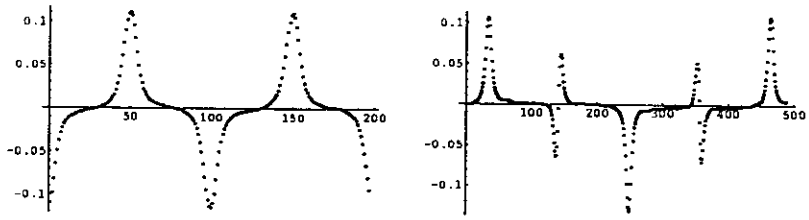


FIGURE 7. Sample data from test stand. Fly height $d = 200$Å.

spacing between samples of $H(x+id)$ is 954Å. With such spacing function $h(x)$, on which or approach is based, has not more than 2 nonzero samples (cf. Figure 3).

## REFERENCES

[1] *Potter R. I.* Analysis of saturation magnetic recording based on arctangent magnetization transition. Journ. appl. phys., **41**(4), 1647–1651 (1974).

[2] *Potter R. I.* Digital magnetic recording theory. IEEE Trans. Magn., MAG-10, 502–508 (1974).

[3] *Heim D. E.* The sensitivity function for shielded magnetoresistive heads by conformal mapping. IEEE Trans. Magn., MAG-19, No.5, 1620–1622 (1983).

[4] *Karlquist O.* Calculation of the magnetic field in the ferromagnetic layer of a magnetic drum. Trans. Royal Inst. Tech. Stockholm, No. 86, 1647–1651 (1954).

[5] *Abramowitz M. and Stegun I.A.* Handbook of mathematical functions, National Bureau of Standards, Applied Mathematics series, **55**, 1964.

[6] *Erdelyi A. and Bateman H.* Higher transcendental functions, McGraw-Hill, London, vol. 3, . 1955.

THEORETICAL PHYSICS DIVISION, NASU INSTITUTE OF MAGNETISM, 36-B VERNADSKY STR., KIEV-680, 252142, UKRAINE

*E-mail address*: dile@imag.kiev.ua